ZOOLOGICAL RESEARCH

Dmrt1 regulates the immune response by repressing the TLR4 signaling pathway in goat male germline stem cells

Yu-Dong Wei[1,#], Xiao-Min Du[1,#], Dong-Hui Yang[1], Fang-Lin Ma[1], Xiu-Wei Yu[1], Meng-Fei Zhang[1], Na Li[1], Sha Peng[1], Ming-Zhi Liao[2], Guang-Peng Li[3], Chun-Ling Bai[3,*], Wei-Shuai Liu[4,*], Jin-Lian Hua[1,*]

[1] *College of Veterinary Medicine*, *Northwest A & F University*, *Shaanxi Centre of Stem Cells Engineering & Technology*, *Yangling*, *Shaanxi* 712100, *China*

[2] *College of Life Sciences*, *Northwest A & F University*, *Yangling*, *Shaanxi* 712100, *China*

[3] *State Key Laboratory of Reproductive Regulation and Breeding of Grassland Livestock*, *School of Life Sciences*, *Inner Mongolia University*, *Hohhot*, *Inner Mongolia* 010021, *China*

[4] *Department of Pathology*, *Yangling Demonstration Zone Hospital*, *Yangling Shaanxi* 712100, *China*

ABSTRACT

Double sex and mab-3-related transcription factor 1 (Dmrt1), which is expressed in goat male germline stem cells (mGSCs) and Sertoli cells, is one of the most conserved transcription factors involved in sex determination. In this study, we highlighted the role of Dmrt1 in balancing the innate immune response in goat mGSCs. Dmrt1 recruited promyelocytic leukemia zinc finger (Plzf), also known as zinc finger and BTB domain-containing protein 16 (Zbtb16), to repress the Toll-like receptor 4 (TLR4)-dependent inflammatory signaling pathway and nuclear factor (NF)-κB. Knockdown of Dmrt1 in seminiferous tubules resulted in widespread degeneration of germ and somatic cells, while the expression of proinflammatory factors were significantly enhanced. We also demonstrated that Dmrt1 stimulated proliferation of mGSCs, but repressed apoptosis caused by the immune response. Thus, Dmrt1 is sufficient to reduce inflammation in the testes, thereby establishing the stability of spermatogenesis and the testicular microenvironment.

Keywords: Male germline stem cells (mGSCs); Goat; Dmrt1; Plzf; Immune response

INTRODUCTION

The innate immune response is a protective reaction against external pathogens. Some organs adopt resistant mechanisms against inflammation congenitally (i.e., mammalian testis, pregnant uterus, eyeball, and brain), which are called immune privileged organs (Chen et al., 2016; Simpson, 2006). Germ cells are protected from pathogens due to the tight junctions between Sertoli cells in seminiferous

Received: 10 December 2020; Accepted: 07 January 2021; Online: 08 January 2021

Foundation items: This work was supported by the China National Basic Research Program (2016YFA0100203), National Natural Science Foundation of China (31572399, 32072806, 32072815, 32002246), State Key Lab of Reproductive Regulation & Breeding of Grassland Livestock (SKL-OT-201801), Science and Technology Major Project of Inner Mongolia Autonomous Region of China (ZDZX2018065), and Shaanxi Province Science and Technology Innovation Team (2019TD-036)

[#]Authors contributed equally to this work

*Corresponding authors, E-mail: chunling1980_0@163.com; liuwei shuaiyou@163.com; jinlianhua@nwsuaf.edu.cn

DOI: 10.24272/j.issn.2095-8137.2020.186

tubules, which allow germ cells to undergo normal spermatogenesis (Hedger, 2012; Inoue et al., 2020; Liang et al., 2019). However, some microbial pathogens can breach the blood-testis barrier (Gimenes et al., 2014; Jia et al., 2017; Ma et al., 2016; Read et al., 2020; Wu et al., 2016; Zeng et al., 2017). Several studies have revealed that transcription factors reduce the immune response. Acetylated promyelocytic leukemia zinc finger (Plzf) recruits a repressor complex consisting of histone deacetylase 3 and nuclear factor (NF)-κB p50 subunits to the promoters of genes containing the NF-κB binding motif (Sadler et al., 2015a, 2015b). Previous study has shown that deficiency of Dmrt1 in male gilthead seabream gonads can lead to a massive infiltration of leukocytes into the testes prior to sex change, suggesting a new role of Dmrt1 that may inhibit the immune response in male gonads (Liarte et al., 2007). Thus, these results suggest the importance of transcription factors in regulating the immune response of germ cells.

Dmrt1 is one of the most conserved transcription factors in a variety of species and is involved in sex determination and germ cell differentiation (Clough et al., 2014; Herpin & Schartl, 2011; Janes et al., 2014; Koopman, 2009; Kopp, 2012; Major & Smith, 2016; Raymond et al., 2000; She & Yang, 2014; Shi et al., 2018). Dmrt1 prevents sexual switch from male to female, represses pluripotency, and balances mitosis versus meiosis (Feng et al., 2014; Griswold et al., 2012; Krentz et al., 2009; Matson et al., 2010; Minkina et al., 2014; Takashima et al., 2013; Zhao et al., 2015). Dmrt1 also maintains spermatogenesis and replenishes mGSCs by collaborating with Plzf and Sal-like protein 4 (Lovelace et al., 2016; Wei et al., 2018; Zhang et al., 2016). These studies illustrate that Dmrt1 generally participates in the development of testicular somatic cells and germ cells.

The innate immune response of testicular germ cells was discovered many years ago. The innate immune response is mainly triggered by Toll-like receptors (TLRs) against invading pathogens (Akira, 2009; De Nardo, 2015; Zhang et al., 2013). TLRs initiate two distinct pathways. The first is the myeloid differentiation protein 88 (MyD88)-dependent pathway, which stimulates NF-κB and mitogen-activated protein kinases (MAPKs) and activates multiple proinflammatory cytokines, including tumor necrosis factor α (TNFα), interleukin 6 (IL-6), and IL-1β (Chen et al., 2016; De Nardo, 2015; Yamamoto & Takeda, 2010). The second is the Toll/IL-1 receptor domain-containing adaptor inducing interferon (IFN)-β-dependent pathway, which up-regulates interferon regulatory factor 3 (IRF3) and activates the expression of IFN-α and IFN-β (Chen et al., 2016; De Nardo, 2015; Yamamoto & Takeda, 2010). In mice, Sertoli cells contain TLR2–TLR6, which initiate innate immune responses and induce the expression of major proinflammatory cytokines. Leydig cells abundantly express TLR2, TLR3, and TLR4. Moreover, TLR3 and TLR4 activation suppresses steroidogenesis in Leydig cells, suggesting innate immune responses may perturb testicular function (Chen et al., 2016). This evidence implies that the innate immune response participates in maintaining homeostasis of the testicular internal environment via testicular somatic cells.

In this study, we highlighted the role of Dmrt1 in balancing the innate immune response in goat male germline stem cells. Our results indicated that Dmrt1 regulated the inflammatory response by repressing TLR4 signaling in goat mGSCs. Transcriptional profiling and dual-luciferase analyses revealed that Dmrt1 recruited Plzf to inhibit the transcriptional activity of TLR4 and NF-κB. Dmrt1 also accelerated spermatogenesis, but decreased apoptosis induced by the immune response, which plays a key role in maintaining the self-renewal and proliferation of mGSCs (Niu et al., 2016; Wei et al., 2018). Our results revealed a new role for Dmrt1 in controlling reproductive immune diseases and maintaining the stability of the testicular microenvironment.

MATERIALS AND METHODS

Ethics approval and consent to participate

All animal experiments were performed in strict accordance with the Guide for the Care and Use of Laboratory Animals (Ministry of Science and Technology of the People's Republic of China, Policy No. 2006398) and were approved by the Animal Care and Use Center of Northwest A & F University (approval No. 201705A299).

Animals and cell culture

Six-month-old Guanzhong dairy goats were selected for the experiments. The animals were kept in an indoor facility located at the Experimental Animal Center of Northwest A&F University.

The procedures for the separation and purification of mGSCs from dairy goats were carried out in accordance with our previous study (Zhu et al., 2012). Briefly, testes from dairy goats were collected aseptically. After washing three times in phosphate-buffered saline (PBS) containing 100 U/mL penicillin and 100 mg/mL streptomycin, the testes were cut into small pieces using sterile scissors. Seminiferous epithelial cells were incubated with an enzyme cocktail containing 0.1% collagenase IV and 10 μg/mL DNase I at 37 °C for 30 min; the cell suspension was blended every 10 min during this period. The dissociated fragments were digested with 0.25% trypsin for 15 min, followed by neutralization with Dulbecco's modified Eagle's medium (DMEM; Invitrogen, USA) supplemented with 10% fetal bovine serum (FBS; HyClone, USA). The suspension was filtered with 40 μm copper mesh to exclude the seminiferous tubules, then plated in plastic culture dishes and incubated in an atmosphere containing 5% CO_2 at 37 °C for 2 h to allow macrophages to attach to the dish. The non-adherent cells were collected and cultured in DMEM/F12 (Invitrogen, USA) containing 10% FBS, 0.1 mmol/L β-mercaptoethanol, 1% non-essential amino acids (Invitrogen, USA), 2 mmol/L L-glutamine (Invitrogen, USA), 10 ng/mL basic fibroblast growth factor (Millipore, USA), 10 ng/mL epidermal growth factor (Millipore, USA), and 10 ng/mL glial-derived neurotrophic factor (Millipore, USA). The cells were cultured for 12 h at 37 °C in an atmosphere of 5% CO_2.

Leydig and Sertoli cells were first adhered to the wall of culture dish. The culture medium for the Leydig cells was the same as that for the mGSCs. Non-adherent cells were obtained and placed into a new dish for culturing at 37 °C in an atmosphere of 5% CO_2. The clones of primary mGSCs were collected after one week.

To prepare the inflammation models, primary mGSC medium supplemented with different lipopolysaccharide (LPS) concentrations (0, 0.5, and 1 μg/mL) (Li et al., 2013) was used for induction. *Capra hircus* adipose mesenchymal stem cells (MSCs) were preserved in our laboratory as a control group. The MSCs and mGSCs were cultured in LPS induction medium to evaluate proliferation and apoptosis.

Immunohistochemical staining was conducted to verify the isolation of mGSCs, Leydig cells, and macrophages using the following primary antibodies: anti-GFRα1 (1 : 500; Santa Cruz Biotechnology, USA), a marker of mGSCs; anti-3β-HSD (1 : 500; Santa Cruz Biotechnology, USA), a marker of Leydig cells; and anti-F4/80 (1 : 100; Proteintech Group, China), a marker of macrophages.

Plasmid construction and lentivirus transfection

The recombinant plasmids pCDH-CMV-MCS-EF1-Dmrt1 (pCDH-Dmrt1), pSIH-H1-shDmrt1 (pSIH-shDmrt1), and pSIH-H1-shTLR4 (pSIH-shTLR4) and assistant plasmids PAX2 and VSVG were stored in our laboratory. For lentivirus preparation, before transfection, the HEK293T cell medium was replaced at 80% confluence. The assistant plasmids PAX2 and VSVG were co-transfected with pCDH-Dmrt1 (or pSIH-shDmrt1 or pSIH-shTLR4) into HEK293T cells at a mass ratio of 3 : 2 : 4. The plasmids supplemented with transfection reagent (TurboFect; Thermo Fisher Scientific, USA) were co-incubated in Opti-MEM (Invitrogen, USA) for 30 min and then added to the HEK293T cell medium. Fresh DMEM/F12 with 2% FBS, 0.1 mmol/L β-mercaptoethanol, 2 mmol/L L-glutamine, 1% non-essential amino acids, and 1% Chemically Defined (CD) lipid (Invitrogen, USA) was added to the infected cells at 12 h after transfection. Lentiviruses pCDH-Dmrt1, pSIH-shDmrt1, and pSIH-shTLR4 were collected after 48 h.

The primary mGSCs were infected with lentivirus pCDH-Dmrt1, pSIH-shDmrt1, or pSIH-shTLR4, complemented with Polybrene (Sigma-Aldrich, USA) to increase transfection efficiency when the cells reached 80% confluence. The infected mGSCs were cultured in medium containing 500 ng/mL puromycin at 37 °C for 1 week to screen for transfection efficiency, and the medium was replaced with fresh DMEM/F12 after 24 h.

Lentivirus injection

Three-month-old ICR male mice purchased from the Fourth Military Medical University in Xi'an, China, were used for lentivirus injection. Mice were deprived of water 12 h before surgery. Tribromoethanol was intraperitoneally injected at 300 mg/kg body weight for anesthesia. The HEK293T cell culture medium was collected as the lentivirus after pSIH-H1 or pSIH-shDmrt1 plasmids were transfected into HEK293T cells after 48 h. The lentivirus was mixed with PEG8000 to condense for 12 h, then centrifuged at 7 000 *g* for 20 min at room temperature. The precipitates were isolated and resuspended in culture medium supplemented with trypan blue. Testes were taken out from a belly wound under aseptic conditions. Efferent ductules were identified under a stereoscope, and the testis was injected with lentivirus through the efferent ductules using a micro-glass pipette (diameter ≤20 μm). For each mouse, the pSIH-shDmrt1 lentivirus was injected directly into the seminiferous tubules of one testis, while the pSIH-H1 lentivirus was injected into the other testis as a control group (Wei et al., 2018). After the operation, the testes were placed back in the scrotum and the wound was sutured. The testes were collected for analysis after 3 weeks. The process for lentivirus injection was approved by the Committee of the Shaanxi Centre of Stem Cells Engineering & Technology, Northwest A&F University.

Immunohistochemical staining

Testes injected with lentivirus were used for immunohistochemical staining. Testes were fixed in a 4% paraformaldehyde solution for 12 h. Gradient dehydration was conducted using 70%, 80%, 90%, and 100% ethanol and xylene I and II. Tissue was embedded in paraffin, cut into 1 mm sections, then placed on slides and dewaxed. Antigens were retrieved with citric acid and the sections were washed three times with PBS. The slides were incubated in 3% H_2O_2 for 10 min at room temperature to block endogenous peroxidase. Mouse primary antibodies were incubated at 37 °C for 2–4 h or at 4 °C overnight. The following antibodies were used for tissue immunohistochemical staining: anti-TLR2 (1 : 200; Santa Cruz Biotechnology, USA), anti-TLR5 (1 : 200; Santa Cruz Biotechnology, USA), anti-TLR4 (1 : 200; Santa Cruz Biotechnology, USA), anti-NF-κB (1 : 200; Santa Cruz Biotechnology, USA), anti-TNFα (1 : 100; Proteintech Group, China), anti-IL-6 (1 : 100; Proteintech Group, China), and anti-F4/80 (1 : 100; Proteintech Group, China). The sections were washed three times with PBS and incubated with secondary antibodies (goat anti-rabbit or goat anti-mouse) conjugated to horseradish peroxidase (HRP) for 1 h at room temperature. The tissues were washed using PBS another three times, after which a DAB chromogenic solution was used to stain the samples. Images were obtained under an EVOS FL fluorescence microscope (AMG, USA).

The tissue immunofluorescence staining procedures followed earlier research (Wei et al., 2018). The antibodies used for tissue immunofluorescence staining included: anti-Dmrt1 (1 : 500; Santa Cruz Biotechnology, USA), anti-Sox9 (1 : 500; Santa Cruz Biotechnology, USA), anti-PCNA (1 : 200; Boster, China), anti-caspase-3 (Biosynthesis Biotechnology, China), anti-ID4 (1 : 100; Boster, China).

For cell immunofluorescence staining, primary mGSCs or LPS-mGSCs were fixed in paraformaldehyde for 15 min at room temperature, and permeabilized with 0.1% Triton-X 100 (Sigma-Aldrich, USA) for 10 min. After blocking for 30 min with 1% bovine serum albumin (Sigma-Aldrich, USA), mGSCs were incubated overnight with primary antibodies anti-TLR4

(1 : 200; Santa Cruz Biotechnology, USA) and anti-NF-κB (1 : 200; Santa Cruz Biotechnology, USA). Secondary antibodies conjugated to fluorescein were applied to the cells for 1 h at room temperature. Nuclei were stained with Hoechst33342 and the cells were washed three times with PBS. Immunofluorescence staining images were captured under an EVOS FL fluorescence microscope (AMG, USA) (Wei et al., 2018).

TAK-242 was purchased from MCE (USA) and dissolved in DMSO. The mGSCs-shDmrt1 were incubated with TAK-242 (100 nmol/L) for two days. Immunofluorescence staining was performed to evaluate the expression of TLR4 and NF-κB in TAK-242-mGSCs-shDmrt1 and shTLR4-mGSCs-shDmrt1, respectively.

Quantitative real-time PCR (qRT-PCR) analysis

The qRT-PCR protocols followed previously described research (Wei et al., 2016). Glyceraldehyde 3-phosphate dehydrogenase (GAPDH) was used as the control gene. Comparative cycle threshold (CT) values from qRT-PCR were used to measure relative gene expression. The primers used for qRT-PCR are shown in Supplementary Table S1.

Western blotting

The western blotting protocols followed previous study (Wei et al., 2016). The primary antibodies used included: anti-Dmrt1 (1 : 500; Santa Cruz Biotechnology, USA), anti-TLR2 (1 : 200; Santa Cruz Biotechnology, USA), anti-TLR5 (1 : 200; Santa Cruz Biotechnology, USA), anti-TLR4 (1 : 200; Santa Cruz Biotechnology, USA), anti-NF-κB (1 : 200; Santa Cruz Biotechnology, USA), anti-TNFα (1 : 100; Proteintech Group, China), anti-IL-6 (1 : 100; Proteintech Group, China), anti-PCNA (1 : 200; Boster, China), anti-inositol-requiring enzyme-1 (IRE1) (Biosynthesis Biotechnology, China), anti-Chop (Biosynthesis Biotechnology, China), anti-p53 (1 : 200; Wanlei Biotechnology, China), anti-cyclin-D1 (1 : 200; Boster, China), anti-Plzf (1 : 300; Sino Biological, China), anti-caspase-3 (Biosynthesis Biotechnology, China), and anti-GAPDH (Tianjin Sungene Biotech, China). Band intensities from three independent experiments were determined by densitometry using NIH ImageJ and the significance of differences was determined by Student's *t*-test.

DMRT1 and PLZF co-immunoprecipitation (co-IP)

Lysates from primary mGSCs were used for IP experiments. Briefly, 500 μg of fresh lysate from different cell treatment groups was incubated with 1 μg of DMRT1 IgG (mouse anti-DMRT1; Santa Cruz Biotechnology, USA), PLZF IgG (rabbit anti-PLZF; Sino Biological, China), or control rabbit IgG (Boster, China) overnight at 4 °C, followed by precipitation with protein A/G-agarose beads (Sigma-Aldrich, USA). Total lysate as input was used as a positive control. Resolution of eluates was determined by polyacrylamide gel electrophoresis (12%) under denaturing SDS (Dmrt1) or denaturing SDS and reducing (Plzf) conditions. The primary antibodies against Dmrt1 and Plzf used for western blotting were the same antibodies used for IP, and the secondary antibodies were conjugated with HRP (Sigma-Aldrich, USA). Results were analyzed using the Tanon-410 automatic gel imaging system (Shanghai Tianneng, China).

Luciferase reporter assay

The luciferase reporter plasmids pGL3-Basic, pGL3-NF-κB, and pCDH-Plzf were stored in the Shaanxi Centre of Stem Cells Engineering & Technology, Northwest A&F University. The vectors were constructed by cloning the promoter of TLR4 into the pGL3-Basic plasmid (Promega, USA). The primers used for TLR4 promoter cloning were F-primer (TAGC TAGCAATATGCTCACGACCTCCG) and R-primer (ATCTCG AGTGCTGTGAGACCAGAGGGG). A total of 50 ng of pGL3-Basic vector or pGL3-TLR4-promoter supplemented with pCDH-Dmrt1 was co-transfected into the mGSCs in a 48-well plate using transfection reagent TurboFect, followed by incubation in Opti-MEM for 30 min at 37 °C. A dual-luciferase reporter system (Beyotime Biotechnology, China) was used to evaluate promoter activity (as determined by fluorescence levels) according to the manufacturer's instructions. Fluorescence levels were assessed using the BHP9504 optical analysis system (Hamamatsu Photonics, Japan) (Wei et al., 2018).

Enzyme-linked immunosorbent assay (ELISA)

The ELISA measurements for GDNF, CSF1, IL-6, and TNFα were conducted as per previous study (Wei et al., 2018) and in accordance with the manufacturer's instructions (Boster, China), with some modification.

Terminal deoxynucleotidyl transferase (TdT)-mediated dUTP-X nicked end labeling (TUNEL)

Mouse testicle slices were used for the TUNEL assay, which was conducted according to the manufacturer's instructions (Vazyme Biotech, China).

Flow cytometry

For cell cycle analysis, mGSCs or MSCs were suspended as single cells, mixed with cold 70% ethanol for 30 min, and incubated with a propidium iodide solution and RNase H for 30 min at room temperature. Flow cytometry was performed to analyze the cell cycle. For each test, three biological replicates were conducted and complied into histogram plots.

Cell apoptosis distribution was assessed after annexin V-FITC and propidium iodide staining. Cells were harvested and washed in cold PBS and cold 1× binding buffer. The cells (1.0×10^5 cells) were re-suspended in cold 1×binding buffer. The cell suspension (100 μL) was added to each labeled tube with 5 μL of annexin V-FITC. The tubes were vortexed gently and incubated for 10 min at room temperature. Propidium iodide solution (5 μL) was added and the tubes were incubated for 5 min at room temperature in the dark. Before analysis, the cells were washed once in PBS and resuspended in PBS. A flow cytometer was utilized to perform the experiment (Beckman Altra; Beckman Coulter, Germany). Fluorescence intensity was also observed under a

fluorescence microscope (Wei et al., 2016). For each test, three biological replicates were conducted and complied into histogram plots.

Cell growth curve

To generate a cell growth curve, primary mGSCs and MSCs were cultured in 24-well plates at a density of 5 000 cells/well. Primary mGSCs and MSCs were exposed to different concentrations of LPS (0, 0.5, and 1 μg/mL) for eight days, and number of cells was counted every day in each group.

Transcriptome sequencing

To assess the molecular regulation of Dmrt1 in mouse testes *in vivo*, control, pSIH-H1, and pSIH-H1-shDmrt1-injected testes with two biological replicates were subjected to transcriptome sequencing. Total RNA was isolated using an RNA Extraction Kit (TaKaRa, China). The amount of RNA was measured by spectrophotometric analysis and its quality was verified by agarose gel electrophoresis. Total RNA (1 μg per sample) was used for cDNA library preparation using a NEB Next Ultra RNA Library Prep Kit (New England BioLabs, USA), and the resulting PCR products were purified and quantified on an Agilent Bioanalyzer 2100 system (New England BioLabs, USA). Sample labeling was performed on a cBot Cluster Generation System using a TruSeq PE Cluster Kit v3-cBot-HS (New England BioLabs, USA). Afterwards, the libraries were sequenced on the Illumina HiSeq PE150 platform (New England BioLabs, USA). Relative gene expression was normalized with the value of reads per kilobase of the exon model per million mapped reads from the mean of two biological replicates in each group (Mortazavi et al., 2008). Genes with a fold-change of ≥2 or ≤0.5 and false discovery rate of <0.01 were considered to have significantly different expression using the DESeq R package. Moreover, Gene Ontology (GO) and Kyoto Encyclopedia of Genes and Genomes (KEGG) enrichment analyses were conducted on the differentially expressed genes (DEGs) using the GO seq R package and KEGG Orthology Based Annotation System (KOBAS) software, respectively (Mortazavi et al., 2008).

Statistical analysis

Two-tailed *t*-tests (Excel, Microsoft 2007) were used to analyze the data. Results are presented as mean±standard deviation (*SD*). All data were obtained from three different experiments and were analyzed by GraphPad Prism software (GraphPad Software, USA) (Wei et al., 2016). *P*-values of <0.05 were considered statistically significant.

RESULTS

Knockdown of Dmrt1 in seminiferous tubules resulted in widespread degeneration of Sertoli cells and inflammation of germ cells

Dmrt1 is mainly located in undifferentiated mGSCs and Sertoli cells, which stimulate differentiation and proliferation, as demonstrated in our previous study (Wei et al., 2018). Dmrt1-knockout male mice show widespread conversion of Sertoli cells into granulosa cells in the seminiferous tubules, where the female sex differentiation gene *Foxl2* is triggered (Minkina et al., 2014; Zhao et al., 2015). However, the characteristics of Dmrt1-deficiency in mGSCs and the testicular niche remain unknown. To solve this problem, we constructed the pSIH-H1-shDmrt1 lentivirus for injection into the seminiferous tubules of mouse testes. Immunofluorescence and hematoxylin and eosin (H&E) staining revealed extensive distribution of inflamed syncytia and widespread degeneration of Sertoli and germ cells in the seminiferous tubules of pSIH-H1-shDmrt1-injected testes (Figure 1A, D; Supplementary Figure S1A, B). Massive structural changes and germ cell loss were also observed (Figure 1A–D; Supplementary Figure S1A, B). Conversely, germ cells were tightly arranged in the control and wild-type groups (Figure 1A–D). These findings were similar to the LPS-infected results (Supplementary Figure S1C). Furthermore, most of the pSIH-H1-shDmrt1-injected testes displayed germ cell degeneration (Supplementary Figure S1D). Thus, we wondered whether this phenotype was due to the deficiency of Dmrt1 in the testicular niche.

Immunohistochemical staining of NF-κB indicated that the positive signal was significantly increased in Dmrt1-knockdown testes (Figure 1E). In addition, staining for proinflammatory cytokines revealed that the syncytia in the seminiferous tubules were positive for IL-6 and TNFα; however, we did not find any pathological changes in the seminiferous tubules of the control and wild-type groups (Figure 1F, G; Supplementary Figure S1C). The levels of IL-6 and TNFα were significantly increased in the Dmrt1-knockdown mouse testes, as measured by ELISA (Figure 1H, I). To confirm these results, qRT-PCR and western blotting were used to examine proinflammatory cytokine levels in the testes of the two groups (Figure 2A–C). Consistent with the staining results, proinflammatory cytokines IL-6, TNFα, IFN-α, IFN-β, IL-8, and TNF receptor-associated factor 3 (Traf3), which are associated with the TLR signaling pathway (De Nardo, 2015), were up-regulated in the shDmrt1 testes in comparison to the control group (Figure 2A). The protein levels of TNFα, NF-κB, and IL-6 were up-regulated as well, suggesting that Dmrt1-knockdown testes suffered severe inflammatory damage (Figure 2B, C). Inflammation is often accompanied by endoplasmic reticulum stress (ERS) and apoptosis in germ cells (Simanjuntak et al., 2018). Our results showed that the expression levels of ERS-related proteins IRE1 and CHOP were increased in the Dmrt1-knockdown testes (Figure 2B, C). These data strongly support the hypothesis that Dmrt1 alleviates ERS induced by inflammation in testicular seminiferous tubules. Immunofluorescence staining and western blotting further revealed that Dmrt1 deficiency increased the apoptosis rate in germ cells but inhibited the proliferation of mGSCs (Figure 2D–F). In general, these results show that Dmrt1 prevents inflammation and apoptosis but promotes mGSC proliferation.

Transcriptional profiling of Dmrt1-knockdown testes

RNA sequencing was conducted to identify the transcriptional

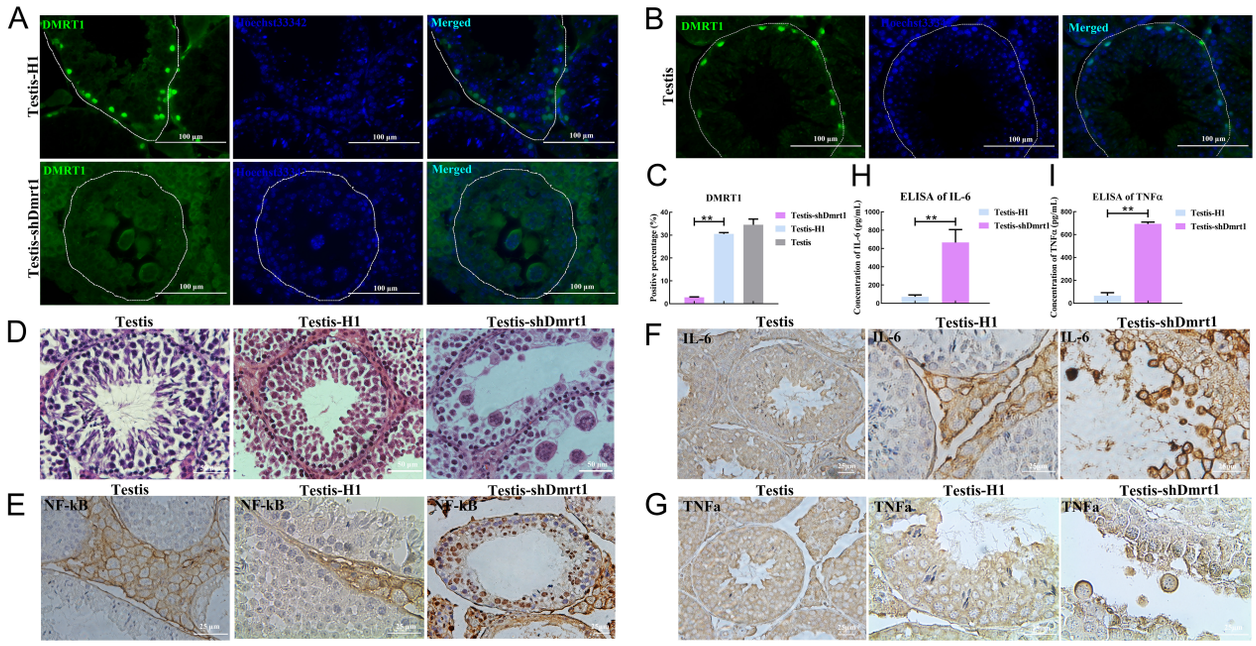

Figure 1 Knockdown of Dmrt1 led to degeneration of spermatogenic cells and inflammation in seminiferous tubules

A: Immunofluorescence staining of Dmrt1 in pSIH-H1-shDmrt1 or pSIH-H1 lentivirus-injected testes. Scale bar: 100 μm. B: Immunofluorescence staining of Dmrt1 in normal mouse testes. Scale bar: 100 μm. C: Percentage of Dmrt1-positive cells in pSIH-H1-shDmrt1 or pSIH-H1 lentivirus-injected testes and normal testes. D: Degeneration of spermatogenic cells in seminiferous tubules following Dmrt1 knockdown. Scale bar: 50 μm. E: Immunohistochemical detection of NF-κB in Dmrt1-knockdown and control testes. Scale bar: 25 μm. F: Immunohistochemical detection of IL-6 in Dmrt1-knockdown and control testes. Scale bar: 25 μm. G: Immunohistochemical detection of TNFα in Dmrt1-knockdown and control testes. Scale bar: 25 μm. H: ELISA of IL-6 in testis-shDmrt1 and testis-H1. I: ELISA of TNFα in testis-shDmrt1 and testis-H1. *: P<0.05; **: P<0.01; ***: P<0.001.

features of testes treated with pSIH-H1-shDmrt1 or pSIH-H1 lentivirus. According to DEG analysis, 1 189 up-regulated and 1 710 down-regulated genes were identified in pSIH-H1-shDmrt1 testes compared with pSIH-H1 testes (Figure 3A). The enriched GO biological processes (P<0.05) revealed that Dmrt1 deficiency affected molecular functions, including oxidation-reduction process, proteolysis, cell adhesion, transmembrane transport, signal transduction, metabolic process, and immune response (Figure 3B; Supplementary Table S2). KEGG pathway annotation and enrichment analysis (P<0.05) showed that Dmrt1-knockdown mediated multiple pathways, including cytokine-cytokine receptor interaction, tuberculosis, phagosome, osteoclast differentiation, amebiasis, and TNF signaling pathway (Figure 3C; Supplementary Table S3). Among the DEGs, Dmrt1 was one of the most differentially expressed. Both Plzf (known also as zinc finger and BTB domain-containing protein 16) and Etv5, which are markers of proliferation in mGSCs, were down-regulated in the pSIH-H1-shDmrt1 testes (Figure 3A; Supplementary Table S4), implying the inhibition of self-renewal in Dmrt1-knockdown testes. However, the most significantly up-regulated genes in the Dmrt1-knockdown group were associated with activation of the inflammatory response. Among them, TLR2, TLR4, TLR6, TLR13, and NF-κB were the most significantly expressed, consistent with our prediction (Figure 3A; Supplementary Table S4).

Taken together, the transcriptome, qRT-PCR, and western blotting data showed that germ cells in Dmrt1-knockdown testes receive deficient self-renewal and proliferation signals from the testicular niche, and an increase in the inflammatory response is a key characteristic in shDmrt1-testes.

TLR4 in mGSCs induced immune response in seminiferous tubules

Transcriptional profiling revealed that genes involved in the TLR signaling pathway were markedly up-regulated, which may be associated with immune response occurrence in Dmrt1-knockdown testes. As TLRs govern the initial stage of inflammation in germ cells, we investigated their expression levels in mGSCs and the mechanism of inflammation in seminiferous tubules. By immunohistochemical staining, we analyzed the profiles of TLR2, TLR4, and TLR5 in pSIH-H1-shDmrt1 testes, which were the most significant DEGs in the TLR family according to the transcriptomic data (Figure 3A). The Dmrt1-knockdown group displayed widespread distribution of TLR4- and TLR2-positive cells in the seminiferous tubules compared with the control group (Supplementary Figure S2A, B). In contrast, TLR5 was barely detected in the germ cells of the shDmrt1 or control testes (Supplementary Figure S2C). Furthermore, double-staining of TLR4 and ID4, markers of spermatogonial stem cells, verified that the TLR4-positive cells were mGSCs (Supplementary Figure S3A).

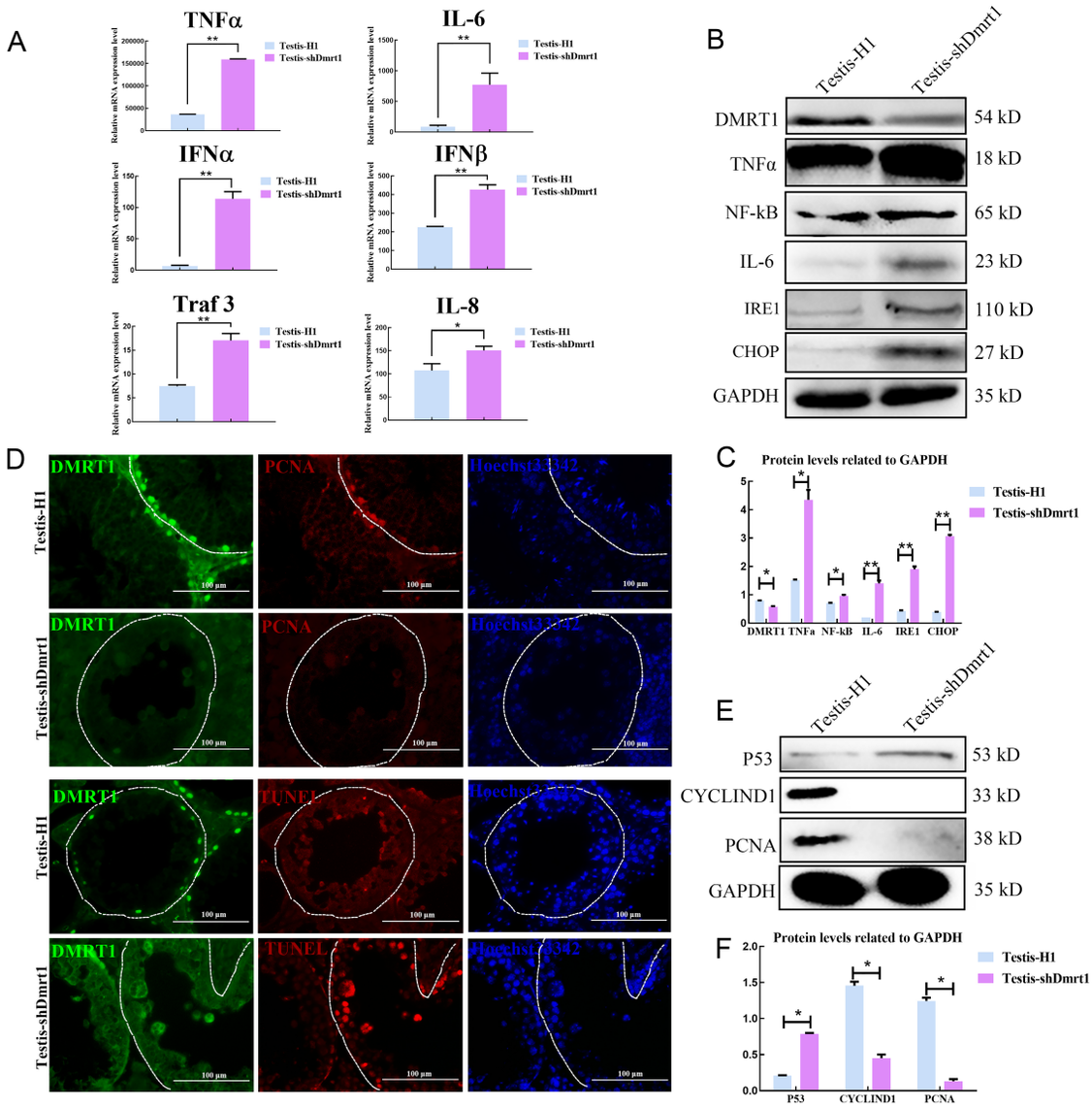

Figure 2 Knockdown Dmrt1 induced apoptosis and reduced proliferation of mGSCs

A: qRT-PCR detection of mRNA levels of inflammatory factors in testis-H1 and testis-shDmrt1. B: Western blotting detection of protein levels of inflammatory factors in testis-H1 and testis-shDmrt1. C: Protein levels were quantified using ImageJ software and normalized to GAPDH. D: Immunofluorescence detection of PCNA and TUNEL assay in testis-H1 and testis-shDmrt1. Scale bar: 100 μm. E: Western blotting detection of protein levels of apoptosis- and proliferation-related genes in testis-H1 and testis-shDmrt1. F: Protein levels were quantified using ImageJ software and normalized to GAPDH. *: $P<0.05$; **: $P<0.01$; ***: $P<0.001$.

To further illustrate that TLR4 was located in the mGSCs, we separated primary mGSCs, Leydig cells, and macrophages from adolescent goat testes *in vitro* (Supplementary Figure S4A); the protocols for mGSC isolation and identification followed our previous study (Zhu et al., 2012). The characteristics of the three types of germ cells were also determined (Supplementary Figure S4B–D). Macrophages play essential roles in the innate immune response, and their numbers increase remarkably to defend against invading pathogens. Therefore, we explored whether the severe inflammation observed in the seminiferous tubules was related to macrophages. However, we did not find distinct differences in the populations of macrophages between the Dmrt1-knockdown and control groups (Supplementary Figure S3B). Thus, we next knocked down Dmrt1 in mGSCs, Leydig cells, and macrophages, respectively, and found that TLR4 expression only increased significantly in the mGSCs (Supplementary Figure S3C). We speculated that TLR4 triggered the immune response in seminiferous tubules when Dmrt1 was deficient in germ cells, and this process was

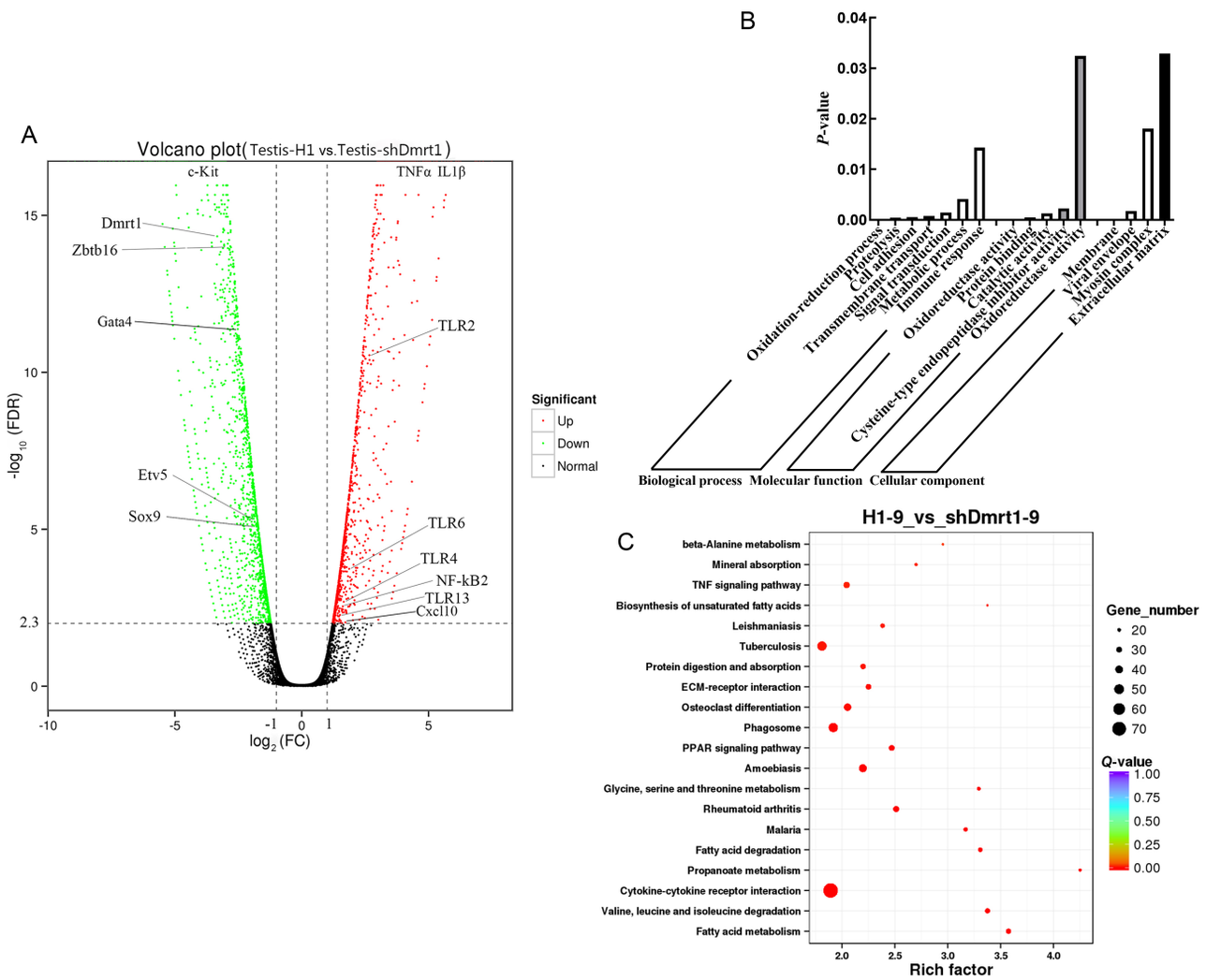

Figure 3 Transcriptional profiling of Dmrt1-knockdown testes

A: Volcano plot of expression profiles comparing testis-H1 and testis-shDmrt1. B: GO analysis of DEGs in testis-H1 and testis-shDmrt1. C: KEGG analysis of DEGs in testis-H1 and testis-shDmrt1.

independent of macrophages.

LPS generally initiates inflammation via TLR4 (Chen et al., 2016; De Nardo, 2015). Here, mGSCs were first treated with 0.5 or 1 μg/mL LPS. Western blotting and qRT-PCR analyses demonstrated that the expression level of TLR4 gradually increased in the LPS treatment group compared with the expression levels of TLR2 and TLR5 (Supplementary Figure S2D–F). These results were consistent with the staining analysis results, which illustrated that TLR4 was mainly located in mGSCs and was responsible for the immune response in seminiferous tubules.

Dmrt1 reduced inflammatory response by inhibiting TLR4 and NF-κB

To further confirm whether Dmrt1 deficiency could account for the increased levels of TLR4 in mGSCs, we analyzed the expression levels of TLR4 and NF-κB in Dmrt1-overexpressed primary mGSCs. Immunofluorescence staining revealed that TLR4 and NF-κB were decreased in the Dmrt1-overexpressed group. Conversely, TLR4- and NF-κB-positive cells were increased when Dmrt1 was knocked down in mGSCs (Figure 4A–C). Moreover, TLR4 antagonist (TAK-242) and lentivirus knockdown of TLR4 also indicated that Dmrt1-knockdown directly induced inflammation through TLR4 and NF-κB signaling (Supplementary Figure S5A–D). To examine this issue, we performed a dual-luciferase reporter assay to test the activity of TLR4 and NF-κB promoters in mGSCs transfected with Dmrt1-overexpressed or Plzf-overexpressed plasmids. Consistent with our expectation, Dmrt1 repressed luciferase activity of the TLR4 and NF-κB promoters (Figure 4D, E). Several studies have demonstrated that Plzf controls the state of chromatin by repressing promoters containing the NF-κB binding motif (Sadler et al., 2015a, 2015b). Here, fluorescence activity of the NF-κB promoter was

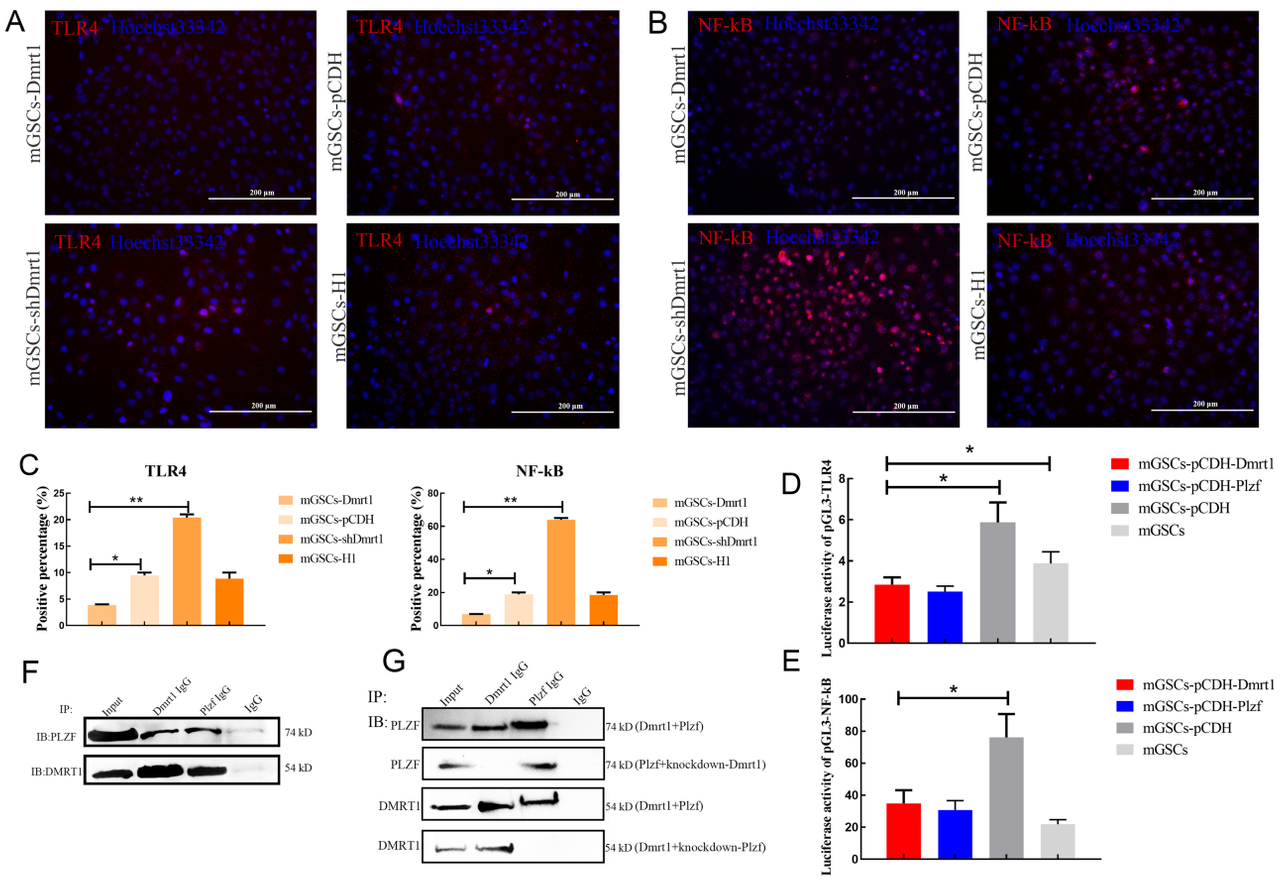

Figure 4 Dmrt1 inhibited TLR4 and NF-kB signaling pathways in mGSCs

A: Immunofluorescence detection of TLR4 in mGSCs-Dmrt1 and mGSCs-shDmrt1. Scale bar: 200 μm. B: Immunofluorescence detection of NF-κB in mGSCs-Dmrt1 and mGSCs-shDmrt1. Scale bar: 200 μm. C: Percentage of TLR4 and NF-κB-positive cells in mGSCs-Dmrt1 and mGSCs-shDmrt1. D: Luciferase activity of pGL3-TLR4 in mGSCs transfected with pCDH-Dmrt1 or pCDH-Plzf, respectively. E: Luciferase activity of pGL3-NF-κB in mGSCs transfected with pCDH-Dmrt1 or pCDH-Plzf, respectively. F: Western blotting for PLZF (top) and DMRT1 (bottom) using IP input lysate and eluates from control IgG, DMRT1 IgG, or PLZF IgG IPs. mGSCs transfected with Dmrt1 plus Plzf-overexpressed plasmids were used for detection. G: Western blotting for PLZF (top) and DMRT1 (bottom) using IP input lysate and eluates from control IgG, DMRT1 IgG, or PLZF IgG IPs. mGSCs transfected with Dmrt1 plus Plzf-overexpressed plasmids, Plzf plus Dmrt1-knockdown plasmids, or Dmrt1 plus Plzf-knockdown plasmids were used for detection. *: P<0.05; **: P<0.01; ***: P<0.001.

decreased in Plzf-overexpressed mGSCs (Figure 4E). We also found that Plzf inhibited the transcriptional activity of TLR4 in mGSCs (Figure 4D). This phenomenon may be due to the interaction between Dmrt1 and Plzf, which enhanced the inhibition of TLR and NF-κB signaling. To validate this, we transfected mGSCs with Dmrt1-overexpressed or Plzf-overexpressed plasmids, and then performed co-IP experiments. While IP for Plzf and Dmrt1 could be selected by individual antibodies, the Dmrt1 IP eluates also contained proteins that cross-reacted with the anti-Plzf antibody (Figure 4F). However, we found no interaction between Dmrt1 IP and the anti-Plzf antibody when Plzf was knocked down (Figure 4G). Together, these data strongly suggest that Dmrt1 interacts with Plzf to reduce the immune response by inhibiting TLR4 and NF-κB signaling.

Dmrt1 inhibited LPS-induced immune response in mGSCs

To further evaluate the underlying mechanism related to the inhibition of the immune response by Dmrt1 *in vitro*, we treated mGSCs with LPS at concentrations of 0, 0.5, and 1 μg/mL. The expression levels of TNFα and IL-6, along with TLR4 and NF-κB, were measured by western blotting. LPS (0.5 and 1 μg/mL) treatment for 12 h resulted in a considerable induction of inflammatory cytokines compared with the control group (Figure 5A, B). To further investigate the role of Dmrt1 in the repression of the immune response, we found that the expression levels of TLR4 and NF-κB were down-regulated in the Dmrt1-overexpressed group (Figure 5C, D). The same results were also obtained by immunofluorescence staining of TLR4 and NF-κB, in which Dmrt1-overexpression decreased the positive signals of TLR4 and NF-κB under LPS induction (Figure 5E–G). Although IL-6

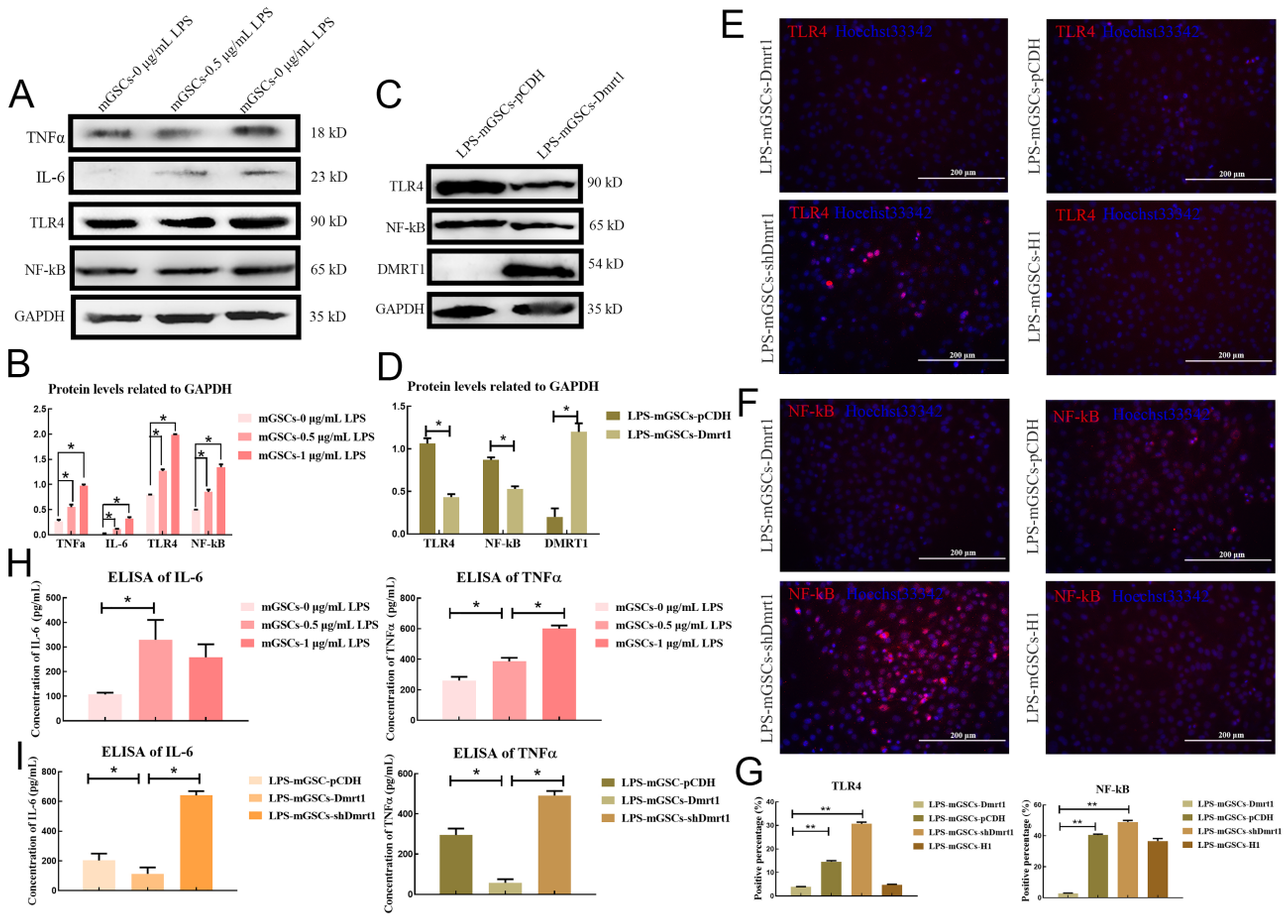

Figure 5 Dmrt1 repressed inflammation induced by LPS in mGSCs

A: Protein expression levels of inflammatory factors TLR4 and NF-κB in mGSCs under treatment with different concentrations of LPS. B: Protein levels were quantified using ImageJ software and normalized to GAPDH. C: Protein expression levels of TLR4, NF-κB, and DMRT1 in LPS-mGSCs-pCDH and LPS-mGSCs-Dmrt1. D: Protein levels were quantified using ImageJ software and normalized to GAPDH. E: Immunofluorescence staining of TLR4 in mGSCs-Dmrt1 and mGSCs-shDmrt1 under LPS treatment. Scale bar: 200 μm. F: Immunofluorescence staining of NF-κB in mGSCs-Dmrt1 and mGSCs-shDmrt1 under LPS treatment. Scale bar: 200 μm. G: Percentage of TLR4- and NF-κB-positive cells in Dmrt1-knockdown or Dmrt1-overexpressed mGSCs. H: ELISA of IL-6 and TNFα in mGSCs under treatment with different concentrations of LPS. I: ELISA of IL-6 and TNFα in mGSCs-Dmrt1 and mGSCs-shDmrt1. *: $P<0.05$; **: $P<0.01$; ***: $P<0.001$.

and TNFα were significantly increased under LPS treatment (Figure 5H), their expression in the Dmrt1-overexpressed group was obviously eliminated (Figure 5I). These data show that Dmrt1 can decrease TLR4 and NF-κB signaling *in vitro*. Our findings also confirmed that Dmrt1 deficiency can promote the transcription of TLR4 and NF-κB, resulting in considerable production of inflammatory cytokines.

Dmrt1 promoted mGSC replenishment against inflammatory injury

Despite initiation of inflammation, LPS also decreases the proliferation of germ cells (Liu et al., 2016). To investigate the effects of LPS on the viability of goat mGSCs, the cell growth curve and population doubling time (PDT) of primary mGSCs challenged with LPS were examined. During this examination, MSCs were used as the control to evaluate the results, as LPS generally increases cell proliferation in MSCs. Results showed that the proliferation rate of mGSCs was inhibited by LPS in a dose-dependent manner, especially in the exponential growth phase, leading to a decrease in the total number of mGSCs (Figure 6A). Flow cytometry analysis also confirmed that mGSCs challenged with 1 μg/mL LPS suffered a severe decline in the DNA duplication rate (S phase) compared with the control group or MSCs (Figure 6B; Supplementary Figure S6A, B). Furthermore, we observed that the apoptosis rate of mGSC-LPS was higher than that of normal mGSCs or MSCs, suggesting that the loss of mGSCs may be due to apoptosis induced by LPS (Figure 6C; Supplementary Figure S6C, D).

We further analyzed the expression levels of cyclin-D1, PCNA, and caspase-3 after LPS treatment. Results showed that LPS indeed induced apoptosis but also suppressed the

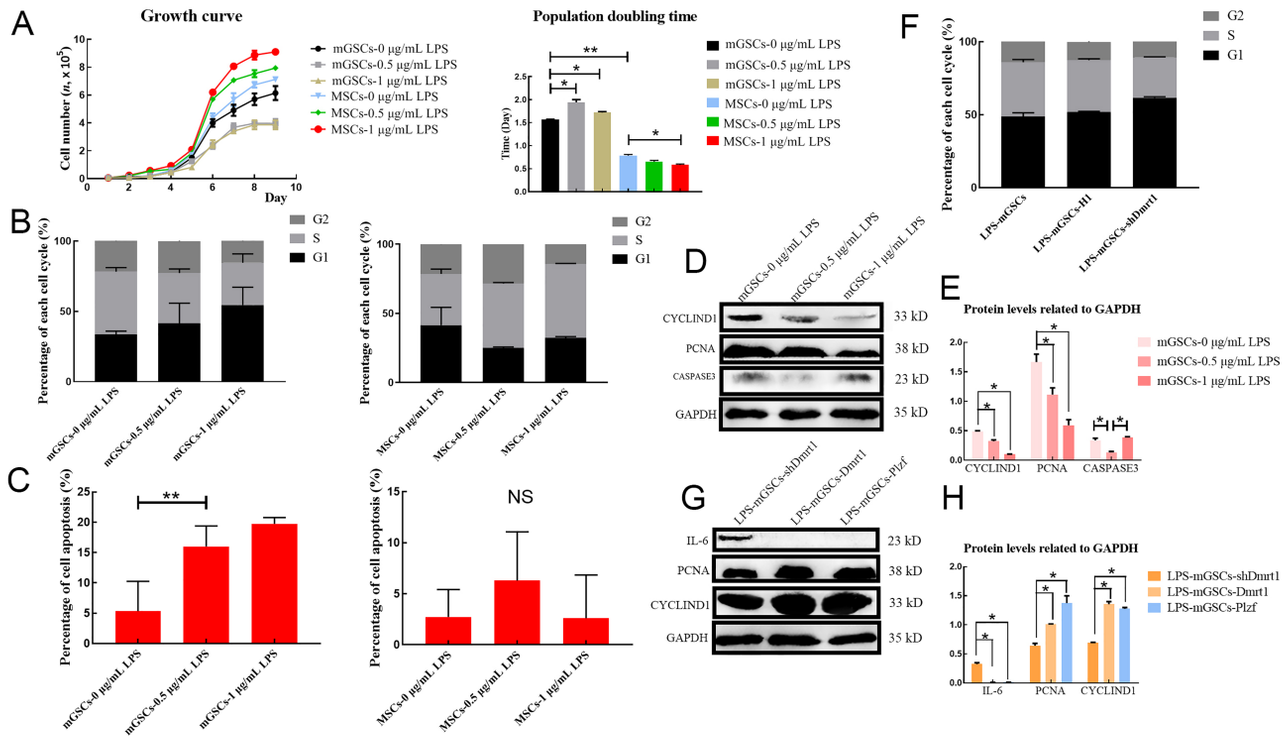

Figure 6 Dmrt1 repressed apoptosis and promoted proliferation of mGSCs

A: Growth curve and population doubling time (PDT) of mGSCs and MSCs under treatment with different concentrations of LPS. B: Flow cytometry of cell cycle in mGSCs and MSCs under LPS treatment (0, 0.5, and 1 μg/mL). C: Flow cytometry of cell apoptosis in mGSCs and MSCs under LPS treatment (0, 0.5, and 1 μg/mL). D: Western blotting of cyclin-D1, PCNA, and caspase-3 in mGSCs under treatment with different concentrations of LPS. E: Protein levels were quantified using ImageJ software and normalized to GAPDH. F: Flow cytometry of cell cycle in LPS-mGSCs, LPS-mGSCs-H1, and LPS-mGSCs-shDmrt1. G: Western blotting of IL-6, PCNA, and cyclin-D1 in LPS-mGSCs-Dmrt1 and LPS-mGSCs-Plzf. H: Protein levels were quantified using ImageJ software and normalized to GAPDH. *: $P<0.05$; **: $P<0.01$; ***: $P<0.001$.

proliferation of goat mGSCs. Cells challenged with 0.5 and 1 μg/mL LPS demonstrated reduced expression levels of cyclin-D1 and PCNA compared with the control group; however, caspase-3 was increased in mGSCs treated with 1 μg/mL LPS, indicating that LPS may trigger the apoptosis pathway (Figure 6D, E).

Previous studies have shown that Dmrt1 promotes the proliferation of male germ cells in testicular damage models by recruiting Plzf (Wei et al., 2018; Zhang et al., 2016). We examined whether Dmrt1 was essential for the preservation of mGSCs under LPS treatment. Flow cytometry was used to test the proliferation rate of mGSCs-shDmrt1 exposed to 1 μg/mL LPS. Consistent with our speculation, the number of cells in the S phase decreased when Dmrt1 was knocked down (Figure 6F; Supplementary Figure S7). However, the protein levels of PCNA and cyclin-D1 were restored in the Dmrt1-overexpressed group (Figure 6G, H). Similar results were also obtained in the mGSCs-Plzf (Figure 6G, H). These results highlighted Dmrt1 and Plzf as key transcription factors in stimulating the self-renewal and proliferation of mGSCs, which promotes the replenishment of these cells during the immune response.

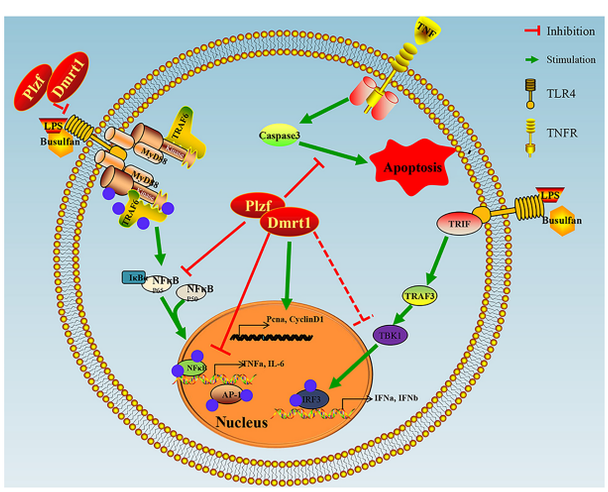

Figure 7 Schematic of Dmrt1 repressing immune response but promoting proliferation of mGSCs

DISCUSSION

Inflammation should be strictly regulated to ensure appropriate immune protection of the host. Defining regulators and their

functions is beneficial to establish effective control over harmful immune responses. Therefore, we demonstrated a crucial role of Dmrt1 in protection against the reproductive immune response. In our Dmrt1-knockdown testis model, the extensive distribution of inflamed syncytia in the center of the seminiferous tubules prompted us to explore the relationship between reproductive immunity and gene therapy. We found that Dmrt1 suppressed infection by directly inhibiting the transcriptional activity of TLR4 and NF-κB. Dmrt1 overexpression in mGSCs led to the restoration of testicular injury and stimulated the differentiation and proliferation of mGSCs by recruiting the transcription factor Plzf.

Self-renewal and proliferation of mGSCs must be maintained for continued mammalian spermatogenesis, and various transcription factors and cytokines involved in this process have been reported (Buaas et al., 2004; Chen et al., 2001, 2005; Falender et al., 2005; Filipponi et al., 2007; Goertz et al., 2011; He et al., 2008; Spradling et al., 2001). Among these transcription factors, Plzf is widely recognized as a key regulator for the preservation of mGSC self-renewal (Costoya et al., 2004; Song et al., 2013), which helps to repair testicular injury. Nevertheless, Plzf also stimulates the development of myeloid tissue and plays a role in the immune response, both of which are important for the development of immune cell lineages crucial for protection against pathogens (Constantinides et al., 2014; Dick & Sergei, 2009; Kovalovsky et al., 2008; Raberger et al., 2008; Savage et al., 2008; Xu et al., 2009). Our data also showed that Plzf suppressed the transcription of TLR4 and NF-κB by binding to specific DNA sequences and contributed to the repair of the testicular niche.

Also known as lipoglycan or endotoxin, LPS is the major component of the outer membrane of gram-negative bacteria. LPS acts as a prototypical endotoxin because it binds to the CD14/TLR4/MD2 receptor complex in many cell types (Dauphinee & Karsan, 2006). LPS triggers the TLR signaling pathway through MyD88 adaptor molecules, resulting in the activation of the NF-κB and MAPK (p38 and ERK) pathways and infected germ cells (Akira & Takeda, 2004; Beutler, 2004; Bhushan et al., 2015). Several transcription factors and molecules that protect germ cells from inflammatory responses have also been reported (Li et al., 2013; Pan et al., 2016; Xie et al., 2017; Zhou et al., 2016). These results suggest the importance of gene therapy in the anti-inflammatory effects of germ cells.

Major testicular cells adopt pattern recognition receptor signaling or TLR signaling to resist inflammation. TLR2 and TLR4 expressed in mouse Sertoli cells induce the expression of major proinflammatory cytokines and type 1 IFNs, whereas most Leydig cells express TLR2, TLR3, and TLR4 (Riccioli et al., 2006; Shang et al., 2011; Wu et al., 2008). Our study revealed that TLR4 was located in the mGSCs. LPS induced the production of IL-6, IL-1β, and TNFα through activation of NF-κB. These germ cells also produced IFN-α and IFN-β, possibly through IRF3 activation, which should be examined in future research. Dmrt1 is distributed in Sertoli and spermatogenic cells, and its expression decreases with the differentiation of mGSCs (Li et al., 2014; Wei et al., 2018; Zhang et al., 2016). However, we observed the expression of TLR2, instead of TLR4, in spermatocytes, which may be involved in other regulatory pathways that are not yet understood. To explore whether Dmrt1 regulates TLR4 and NF-κB directly, we conducted a dual-luciferase assay and revealed that Dmrt1 was bound to the promoters of TLR4 and NF-κB. However, Dmrt1 binding motif identification, chromatin immunoprecipitation, and chromatin immunoprecipitation sequencing should be performed to verify our findings.

Dmrt1 plays a variety of roles in Sertoli and germ cells, e.g., male maintenance, germ cell maturation, apoptosis regulation, and male determination (Clough et al., 2014; Herpin & Schartl, 2011; Janes et al., 2014; Koopman, 2009; Kopp, 2012; Major & Smith, 2016; Raymond et al., 2000; She & Yang, 2014; Shi et al., 2018). The decrease in Dmrt1 in testes may lead to significant changes in Sertoli cell function or sex reversal. The increase in testicular inflammatory response may also be due to the degeneration of Sertoli cells, which may explain how the absence of Dmrt1 promotes inflammation. However, this subject needs further exploration.

Our previous research demonstrated that Dmrt1 induces a self-repair ability in busulfan-treated testes, in which germ cells are damaged by DNA alkylation (Wei et al., 2018). Here, the recruitment of Plzf by Dmrt1 also contributed to the replenishment of mGSCs. Furthermore, Dmrt1-knockdown resulted in the substantial production of inflammatory cytokines *in vitro* and *in vivo*, while overexpression of Dmrt1 replenished male germ cells in the LPS treatment group. In the current study, we tested the hypothesis that Dmrt1 is essential for reducing inflammation in goat germ cells, thereby establishing the stability of spermatogenesis and the testicular microenvironment. For the first time, the effects of Dmrt1 in protecting against the immune response in mammalian mGSCs were investigated (Figure 7).

SUPPLEMENTARY DATA

Supplementary data to this article can be found online.

COMPETING INTERESTS

The authors declare that they have no competing interests.

AUTHORS' CONTRIBUTIONS

Y.D.W. and J.L.H. designed the research. Y.D.W., X.M.D., D.H.Y., and X.W.Y. performed most of the research; X.W.Y., F.L.M., and M.F.Z. contributed to lentivirus injection and the mouse model; Y.D.W., S.P., and J.L.H. analyzed the data. Y.D.W. and J.L.H. wrote the paper. Y.D.W., N. L, G.P.L., C.L.B., M.Z.L., W.S.L., and J.L.H. revised the paper. All authors read and approved the final version of the manuscript.

ACKNOWLEDGMENTS

The authors thank Dr. John Clotaire Daguia Zambe for helpful comments about this paper, Jia Fang for the PGL3-NF-κB luciferase reporter plasmid, and Dong-Xue Che for bioinformatics analysis.

REFERENCES

Akira S. 2009. Pathogen recognition by innate immunity and its signaling. *Proceedings of the Japan Academy, Series B*, **85**(4): 143−156.

Akira S, Takeda K. 2004. Toll-like Receptor Signalling. New York: Cold Spring Harbor Laboratory Press.

Beutler B. 2004. Inferences, questions and possibilities in toll-like receptor signalling. *Nature*, **430**(6996): 257−263.

Bhushan S, Tchatalbachev S, Lu YN, Fröhlich S, Fijak M, Vijayan V, et al. 2015. Differential activation of inflammatory pathways in testicular macrophages provides a rationale for their subdued inflammatory capacity. *Journal of Immunology*, **194**(11): 5455−5464.

Buaas FW, Kirsh AL, Sharma M, Mclean DJ, Morris JL, Griswold MD, et al. 2004. *Plzf* is Required in Adult Male Germ Cells for Stem Cell Self-Renewal. New York: Humana Press.

Chen C, Ouyang W, Grigura V, Zhou Q, Carnes K, Lim H, et al. 2005. ERM is required for transcriptional control of the spermatogonial stem cell niche. *Nature*, **436**(7053): 1030−1034.

Chen QY, Deng TT, Han DS. 2016. Testicular immunoregulation and spermatogenesis. *Seminars in Cell & Developmental Biology*, **59**: 157−165.

Chen WS, Xu PZ, Gottlob K, Chen ML, Sokol K, Shiyanova T, et al. 2001. Growth retardation and increased apoptosis in mice with homozygous disruption of the *akt1* gene. *Genes & Development*, **15**(17): 2203−2208.

Clough E, Jimenez E, Kim YA, Whitworth C, Neville MC, Hempel L, et al. 2014. Sex- and tissue-specific functions of *Drosophila* doublesex transcription factor target genes. *Developmental Cell*, **31**(6): 761−773.

Constantinides MG, McDonald BD, Verhoef PA, Bendelac A. 2014. A committed precursor to innate lymphoid cells. *Nature*, **508**(7496): 397−401.

Costoya JA, Hobbs RM, Barna M, Cattoretti G, Manova K, Sukhwani M, et al. 2004. Essential role of Plzf in maintenance of spermatogonial stem cells. *Nature Genetics*, **36**(6): 653−659.

Dauphinee SM, Karsan A. 2006. Lipopolysaccharide signaling in endothelial cells. *Laboratory Investigation*, **86**(1): 9−22.

De Nardo D. 2015. Toll-like receptors: activation, signalling and transcriptional modulation. *Cytokine*, **74**(2): 181−189.

Dick JE, Sergei D. 2009. The role of PLZF in human myeloid development. *Annals of the New York Academy of Sciences*, **1176**(1): 150−153.

Falender AE, Freiman RN, Geles KG, Lo KC, Hwang KS, Lamb DJ, et al. 2005. Maintenance of spermatogenesis requires TAF4B, a gonad-specific subunit of TFIID. *Genes & Development*, **19**(7): 794−803.

Feng CW, Bowles J, Koopman P. 2014. Control of mammalian germ cell entry into meiosis. *Molecular and Cellular Endocrinology*, **382**(1): 488−497.

Filipponi D, Hobbs RM, Ottolenghi S, Rossi P, Jannini EA, Pandolfi PP, et al. 2007. Repression of kit expression by Plzf in germ cells. *Molecular and Cellular Biology*, **27**(19): 6770−6781.

Gimenes F, Souza RP, Bento JC, Teixeira JJV, Maria-Engler SS, Bonini MG, et al. 2014. Male infertility: a public health issue caused by sexually transmitted pathogens. *Nature Reviews Urology*, **11**(12): 672−687.

Goertz MJ, Wu ZR, Gallardo TD, Hamra FK, Castrillon DH. 2011. Foxo1 is required in mouse spermatogonial stem cells for their maintenance and the initiation of spermatogenesis. *Journal of Clinical Investigation*, **121**(9): 3456−3466.

Griswold MD, Hogarth CA, Bowles J, Koopman P. 2012. Initiating meiosis: the case for retinoic acid. *Biology of Reproduction*, **86**(2): 35.

He Z, Jiang J, Kokkinaki M, Golestaneh N, Hofmann MC, Dym M. 2008. GDNF upregulates *c*-fos transcription via the Ras/ERK1/2 pathway to promote mouse spermatogonial stem cell proliferation. *Stem Cells*, **26**(1): 266−278.

Hedger MP. 2012. Immune privilege of the testis: meaning, mechanisms, and manifestations. *In*: Stein-Streilein J. Infection, Immune Homeostasis and Immune Privilege. Basel: Springer.

Herpin A, Schartl M. 2011. *Dmrt1* genes at the crossroads: a widespread and central class of sexual development factors in fish. *FEBS Journal*, **278**(7): 1010−1019.

Inoue T, Aoyama-Ishikawa M, Uemura M, Yamashita H, Koga Y, Terashima M, et al. 2020. Interleukin-18 levels and mouse leydig cell apoptosis during lipopolysaccharide-induced acute inflammatory conditions. *Journal of Reproductive Immunology*, **141**: 103167.

Janes DE, Organ CL, Stiglec R, O'meally D, Sarre SD, Georges A, et al. 2014. Molecular evolution of *Dmrt1* accompanies change of sex-determining mechanisms in reptilia. *Biology Letters*, **10**(12): 20140809.

Jia XY, Xu Y, Wu WX, Fan YX, Wang GL, Zhang TB, et al. 2017. Aroclor1254 disrupts the blood-testis barrier by promoting endocytosis and degradation of junction proteins via p38 MAPK pathway. *Cell Death & Disease*, **8**(5): e2823.

Koopman P. 2009. Sex determination: the power of *DMRT1*. *Trends in Genetics*, **25**(11): 479−481.

Kopp A. 2012. *Dmrt* genes in the development and evolution of sexual dimorphism. *Trends in Genetics*, **28**(4): 175−184.

Kovalovsky D, Uche OU, Eladad S, Hobbs RM, Yi W, Alonzo E, et al. 2008. The BTB-zinc finger transcriptional regulator PLZF controls the development of invariant natural killer T cell effector functions. *Nature Immunology*, **9**(9): 1055−1064.

Krentz AD, Murphy MW, Kim S, Cook MS, Capel B, Zhu R, et al. 2009. The DM domain protein DMRT1 is a dose-sensitive regulator of fetal germ cell proliferation and pluripotency. *Proceedings of the National Academy of Sciences of the United States of America*, **106**(52): 22323−22328.

Li L, Ma P, Liu YJ, Huang C, O WS, Tang F, et al. 2013. Intermedin attenuates LPS-induced inflammation in the rat testis. *PLoS One*, **8**(6): e65278.

Li XY, Li Z, Zhang XJ, Zhou L, Gui JF. 2014. Expression characterization of testicular DMRT1 in both sertoli cells and spermatogenic cells of polyploid gibel carp. *Gene*, **548**(1): 119−125.

Liang JL, Wang N, He J, Du J, Guo YH, Li L, et al. 2019. Induction of sertoli-like cells from human fibroblasts by NR5A1 and GATA4. *eLife*, **8**: e48767.

Liarte S, Chaves-Pozo E, García-Alcazar A, Mulero V, Meseguer J, García-Ayala A. 2007. Testicular involution prior to sex change in gilthead seabream is characterized by a decrease in DMRT1 gene expression and by massive leukocyte infiltration. *Reproductive Biology and Endocrinology*, **5**(1): 20.

Liu XR, Wang YY, Dan XG, Kumar A, Ye TZ, Yu YY, et al. 2016. Anti-inflammatory potential of β-cryptoxanthin against LPS-induced inflammation in mouse sertoli cells. *Reproductive Toxicology*, **60**: 148−155.

Lovelace DL, Gao Z, Mutoji K, Song YC, Ruan JH, Hermann BP. 2016. The regulatory repertoire of PLZF and SALL4 in undifferentiated spermatogonia. *Development*, **143**(11): 1893−1906.

Ma WQ, Li SH, Ma SQ, Jia L, Zhang FC, Zhang Y, et al. 2016. Zika virus causes testis damage and leads to male infertility in mice. *Cell*, **167**(6): 1511−1524.

Major AT, Smith CA. 2016. Sex reversal in birds. *Sexual Development*, **10**(5–6): 288−300.

Matson CK, Murphy MW, Griswold MD, Yoshida S, Bardwell VJ, Zarkower D. 2010. The mammalian doublesex homolog DMRT1 is a transcriptional gatekeeper that controls the mitosis versus meiosis decision in male germ cells. *Developmental Cell*, **19**(4): 612−624.

Minkina A, Matson CK, Lindeman RE, Ghyselinck NB, Bardwell VJ, Zarkower D. 2014. DMRT1 protects male gonadal cells from retinoid-dependent sexual transdifferentiation. *Developmental Cell*, **29**(5): 511−520.

Mortazavi A, Williams BA, McCue K, Schaeffer L, Wold B. 2008. Mapping and quantifying mammalian transcriptomes by RNA-Seq. *Nature Methods*, **5**(7): 621−628.

Niu BW, Li B, Wu CY, Wu J, Yan Y, Shang R, et al. 2016. Melatonin promotes goat spermatogonia stem cells (SSCs) proliferation by stimulating glial cell line-derived neurotrophic factor (GDNF) production in Sertoli cells. *Oncotarget*, **7**(47): 77532−77542.

Pan YQ, Liu Y, Wang L, Xue F, Hu YQ, Hu R, et al. 2016. MKP-1 attenuates LPS-induced blood-testis barrier dysfunction and inflammatory response through p38 and IκBα pathways. *Oncotarget*, **7**(51): 84907−84923.

Raberger J, Schebesta A, Sakaguchi S, Boucheron N, Blomberg KE, Berglöf A, et al. 2008. The transcriptional regulator PLZF induces the development of CD44 high memory phenotype T cells. *Proceedings of the National Academy of Sciences of the United States of America*, **105**(46): 17919−17924.

Raymond CS, Murphy MW, O'Sullivan MG, Bardwell VJ, Zarkower D. 2000. *Dmrt1*, a gene related to worm and fly sexual regulators, is required for mammalian testis differentiation. *Genes & Development*, **14**(20): 2587−2595.

Read AJ, Gestier S, Parrish K, Finlaison DS, Gu XN, O'Connor TW, et al. 2020. Prolonged detection of bovine viral diarrhoea virus infection in the semen of bulls. *Viruses*, **12**(6): 674.

Riccioli A, Starace D, Galli R, Fuso A, Scarpa S, Palombi F, et al. 2006. Sertoli cells initiate testicular innate immune responses through TLR activation. *The Journal of Immunology*, **177**(10): 7122−7130.

Sadler AJ, Rossello FJ, Yu L, Deane JA, Yuan XL, Wang D, et al. 2015a. BTB-ZF transcriptional regulator PLZF modifies chromatin to restrain inflammatory signaling programs. *Proceedings of the National Academy of Sciences of the United States of America*, **112**(5): 1535−1540.

Sadler AJ, Suliman BA, Yu L, Yuan XL, Wang D, Irving AT, et al. 2015b. The acetyltransferase HAT1 moderates the NF-κB response by regulating the transcription factor PLZF. *Nature Communications*, **6**: 6795.

Savage AK, Constantinides MG, Han J, Picard D, Martin E, Li BF, et al. 2008. The transcription factor PLZF directs the effector program of the NKT cell lineage. *Immunity*, **29**(3): 391−403.

Shang T, Zhang XY, Wang T, Sun B, Deng TT, Han DS. 2011. Toll-like receptor-initiated testicular innate immune responses in mouse leydig cells. *Endocrinology*, **152**(7): 2827−2836.

She ZY, Yang WX. 2014. Molecular mechanisms involved in mammalian primary sex determination. *Journal of Molecular Endocrinology*, **53**(1): R21−R37.

Shi WJ, Jiang YX, Huang GY, Zhao JL, Zhang JN, Liu YS, et al. 2018. Dydrogesterone causes male bias and accelerates sperm maturation in zebrafish (*Danio rerio*). *Environmental Science & Technology*, **52**(15): 8903−8911.

Simanjuntak Y, Liang JJ, Chen SY, Li JK, Lee YL, Wu HC, et al. 2018. Ebselen alleviates testicular pathology in mice with Zika virus infection and prevents its sexual transmission. *PLoS Pathogens*, **14**(2): e1006854.

Simpson E. 2006. A historical perspective on immunological privilege. *Immunological Reviews*, **213**(1): 12−22.

Song W, Zhu H, Li M, Li N, Wu J, Mu H, et al. 2013. Promyelocytic leukaemia zinc finger maintains self-renewal of male germline stem cells (mGSCs) and its expression pattern in dairy goat testis. *Cell Proliferation*, **46**(4): 457−468.

Spradling A, Drummond-Barbosa D, Kai T. 2001. Stem cells find their niche. *Nature*, **414**(6859): 98−104.

Takashima S, Hirose M, Ogonuki N, Ebisuya M, Inoue K, Kanatsu-Shinohara M, et al. 2013. Regulation of pluripotency in male germline stem cells by Dmrt1. *Genes & Development*, **27**(18): 1949−1958.

Wei YD, Cai SF, Ma FL, Zhang Y, Zhou Z, Xu SS, et al. 2018. Double sex and mab-3 related transcription factor 1 regulates differentiation and proliferation in dairy goat male germline stem cells. *Journal of Cellular Physiology*, **233**(3): 2537−2548.

Wei YD, Fang J, Cai SF, Lv CR, Zhang SQ, Hua J. 2016. Primordial germ cell–like cells derived from canine adipose mesenchymal stem cells. *Cell Proliferation*, **49**(4): 503−511.

Wu H, Shi LL, Wang Q, Cheng LJ, Zhao X, Chen QY, et al. 2016. Mumps virus-induced innate immune responses in mouse sertoli and leydig cells. *Scientific Reports*, **6**: 19507.

Wu H, Wang HK, Xiong WP, Chen S, Tang HM, Han DS. 2008. Expression patterns and functions of toll-like receptors in mouse sertoli cells. *Endocrinology*, **149**(9): 4402−4412.

Xie TC, Hu GH, Dong BB, Yan YY, Liu M, Yao XD, et al. 2017. Roscovitine protects murine leydig cells from lipopolysaccharide-induced inflammation. *Experimental and Therapeutic Medicine*, **13**(5): 2169−2176.

Xu DK, Holko M, Sadler AJ, Scott B, Higashiyama S, Berkofsky-Fessler W, et al. 2009. Promyelocytic leukemia zinc finger protein regulates interferon-mediated innate immunity. *Immunity*, **30**(6): 802−816.

Yamamoto M, Takeda K. 2010. Current views of toll-like receptor signaling pathways. *Gastroenterology Research and Practice*, **2010**: 240365.

Zeng XK, Blancett CD, Koistinen KA, Schellhase CW, Bearss JJ, Radoshitzky SR, et al. 2017. Identification and pathological characterization of persistent asymptomatic Ebola virus infection in rhesus monkeys. *Nature Microbiology*, **2**(9): 17113.

Zhang T, Oatley J, Bardwell VJ, Zarkower D. 2016. DMRT1 is required for mouse spermatogonial stem cell maintenance and replenishment. *PLoS Genetics*, **12**(9): e1006293.

Zhang XY, Wang T, Deng TT, Xiong WP, Lui P, Li N, et al. 2013. Damaged spermatogenic cells induce inflammatory gene expression in mouse sertoli cells through the activation of toll-like receptors 2 and 4. *Molecular and Cellular Endocrinology*, **365**(2): 162−173.

Zhao L, Svingen T, Ng ET, Koopman P. 2015. Female-to-male sex reversal in mice caused by transgenic overexpression of *Dmrt1*. *Development*, **142**(6): 1083−1088.

Zhou PH, Hu W, Zhang XB, Wang W, Zhang LJ. 2016. Protective effect of adrenomedullin on rat leydig cells from lipopolysaccharide-induced inflammation and apoptosis via the PI3K/Akt signaling pathway ADM on rat leydig cells from inflammation and apoptosis. *Mediators of Inflammation*, **2016**: 7201549.

Zhu H, Liu C, Sun J, Li M, Hua J. 2012. Effect of GSK-3 inhibitor on the proliferation of multipotent male germ line stem cells (mGSCs) derived from goat testis. *Theriogenology*, **77**(9): 1939−1950.